Electronic Supplementary Information (ESI)

Ag Nanocrystal as a Promoter for Carbon Nanotube-based Room-temperature Gas Sensors

Shumao Cui,[a,§] Haihui Pu,[a,§]. Eric C. Mattson,[b] Ganhua Lu,[a] Shun Mao,[a] Michael Weinert,[b] Carol J. Hirschmugl,[b] Marija Gajdardziska-Josifovska,[b] Junhong Chen[a,*]

[a]Department of Mechanical Engineering, University of Wisconsin-Milwaukee, 3200 N Cramer Street, Milwaukee, WI, 53211, USA.

[b]Department of Physics and Laboratory for Surface Studies, University of Wisconsin-Milwaukee, 1900 E. Kenwood Blvd, Milwaukee, WI, 53211, USA.

*Corresponding author email: jhchen@uwm.edu

§ These authors contributed equally.

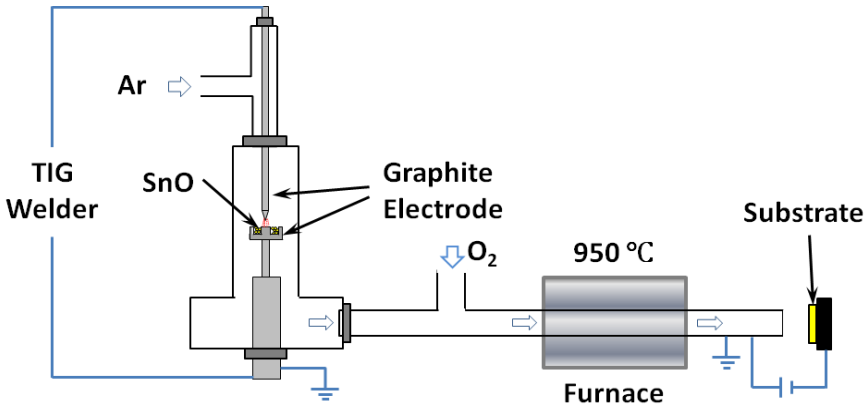

Fig. S1 Schematic setup of SnO_2 nanoparticle synthesis system.

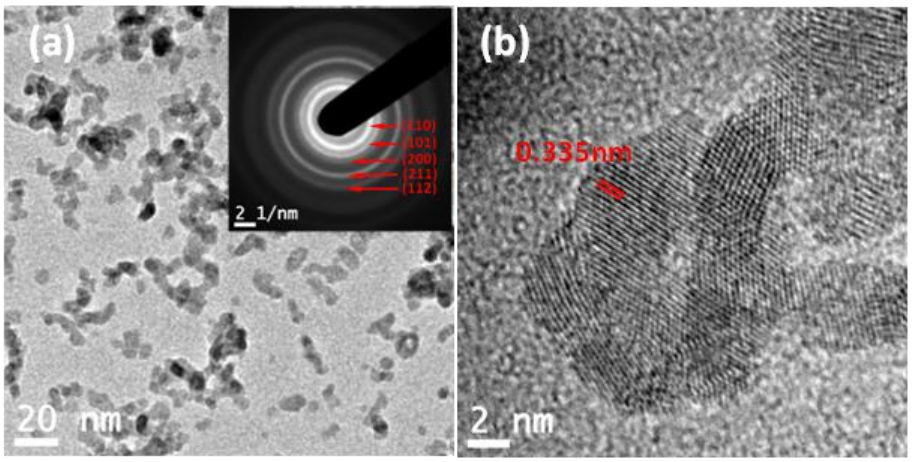

Fig. S2 (a) Low magnification TEM image and SAED pattern (inset) of SnO_2 nanoparticles synthesized at 950 °C. (b) HRTEM image of SnO_2 nanoparticles. 0.335 nm lattice spacing is indexed to (110) plane of rutile SnO_2.

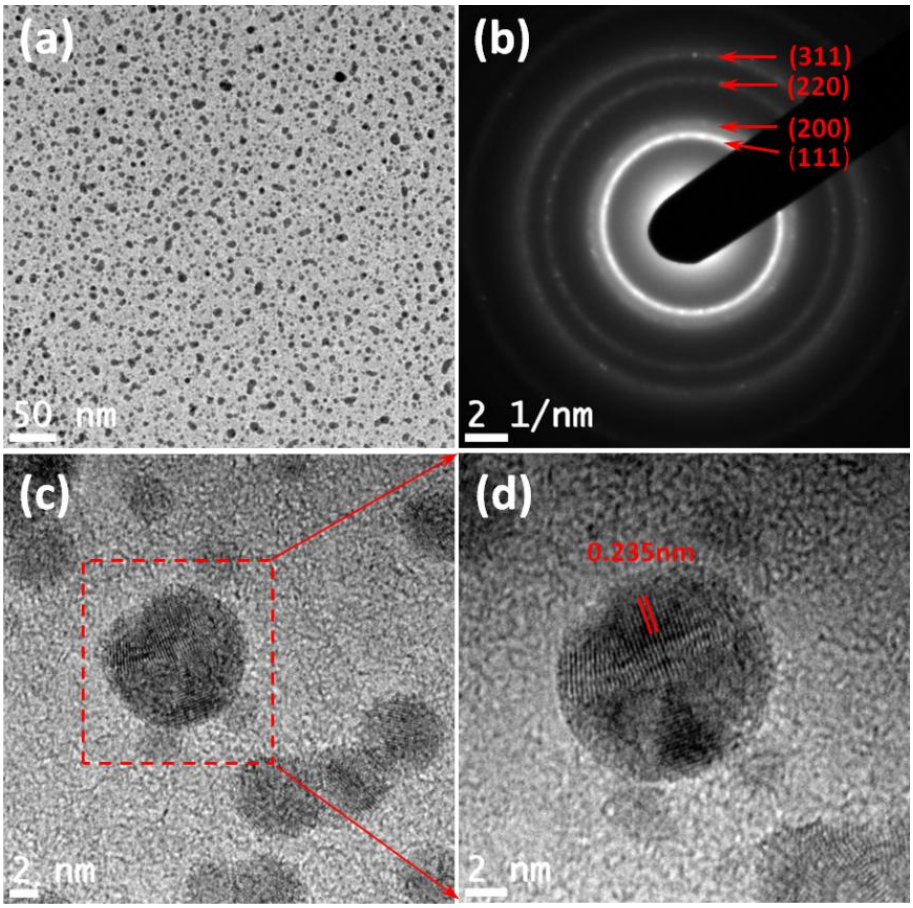

Fig. S3 Low magnification TEM image (a) and SAED pattern (b) of as-produced Ag NPs. (c), and (d) HRTEM images of Ag NPs, and 0.235 nm lattice spacing is indexed to (111) plane of Ag.

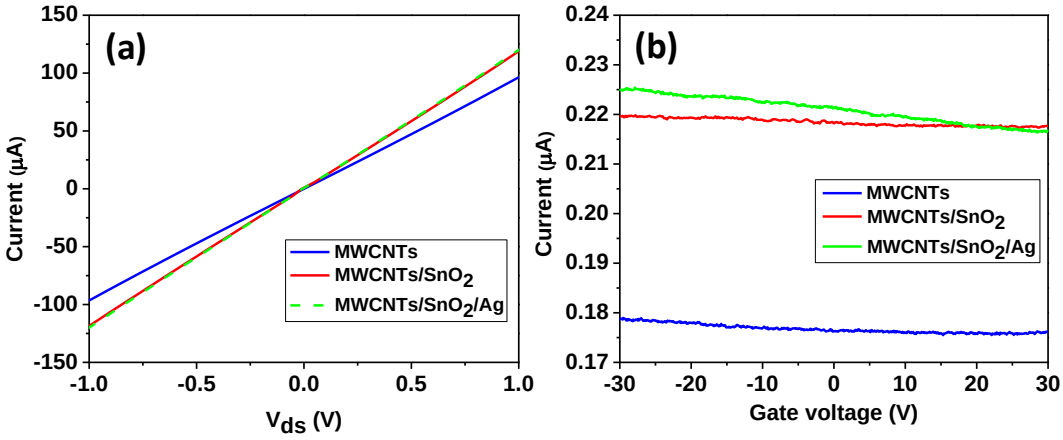

Fig. S4 (a) *I-V* curve evolution of MWCNTs at different conditions (with and without NP coating). (b) The dependence of current on gate voltage.

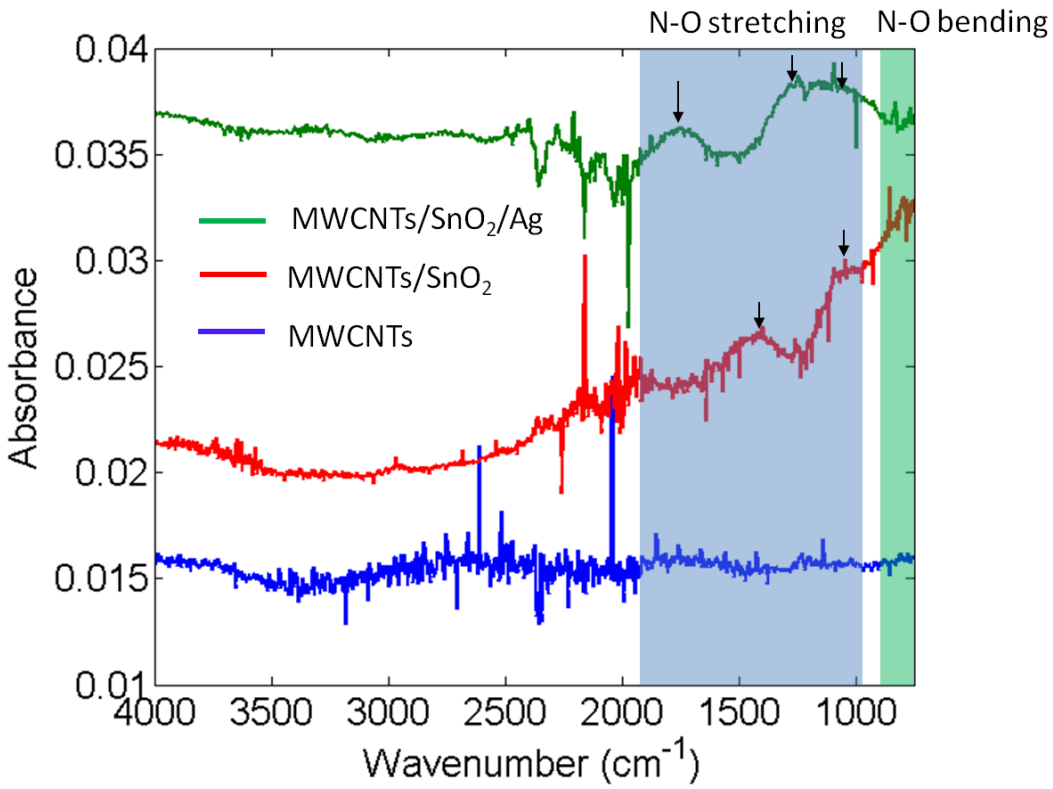

Fig. S5 Differential IR absorbance spectra of MWCNT hybrid sensors exposed to100 ppm NO_2 diluted in Ar.

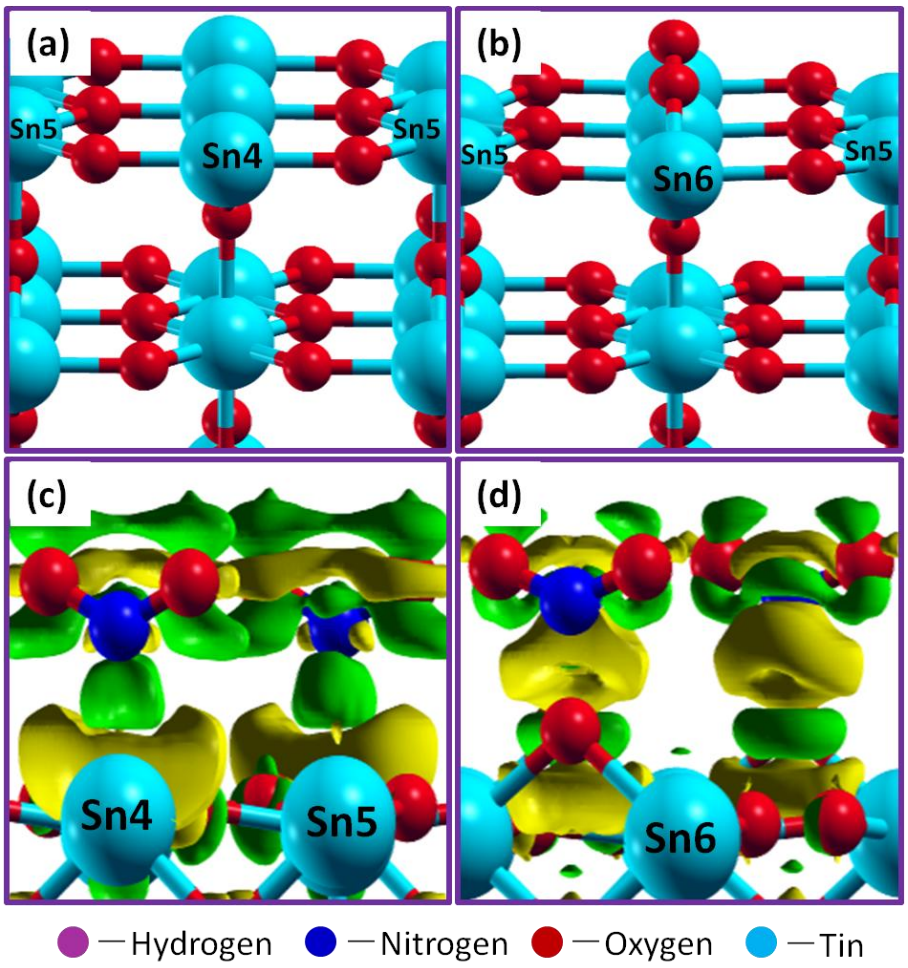

Fig. S6 Upper panel: Perspective views of the SnO_2 (110) surface with the coordination number of different Sn atoms labeled, (a) planar-reduced surface and (b) oxidized surface with oxygen atoms sitting on the bridge sites. Lower panel: Charge density difference upon NO_2 molecule adsorption on the surface. Green and yellow represent electron accumulation and depletion regions, respectively. (c) NO_2 is attracted directly to the Sn4 atom with gain of 0.0576 e^-. (d) NO_2 forms $NO_3^{\delta-}$ complex with gain of 0.0069 e^-. For NH_3 adsorption, it prefers the Sn5 site instead of the bridging oxygen. However, this site is preoccupied by O_2 at room temperature and leads to the reluctance of sensor to NH_3.

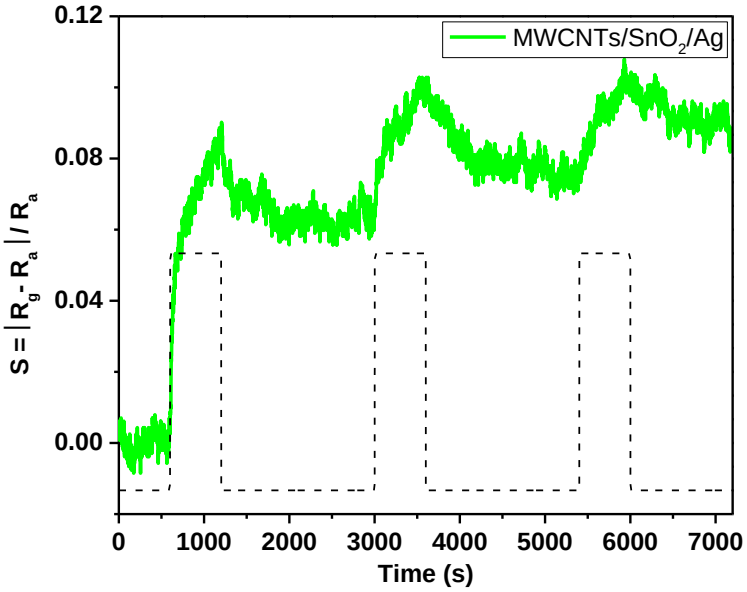

Fig. S7 Representative sensing response of Ag/SnO_2/MWCNTs hybrid structures to 100 ppm NO_2 at room temperature.

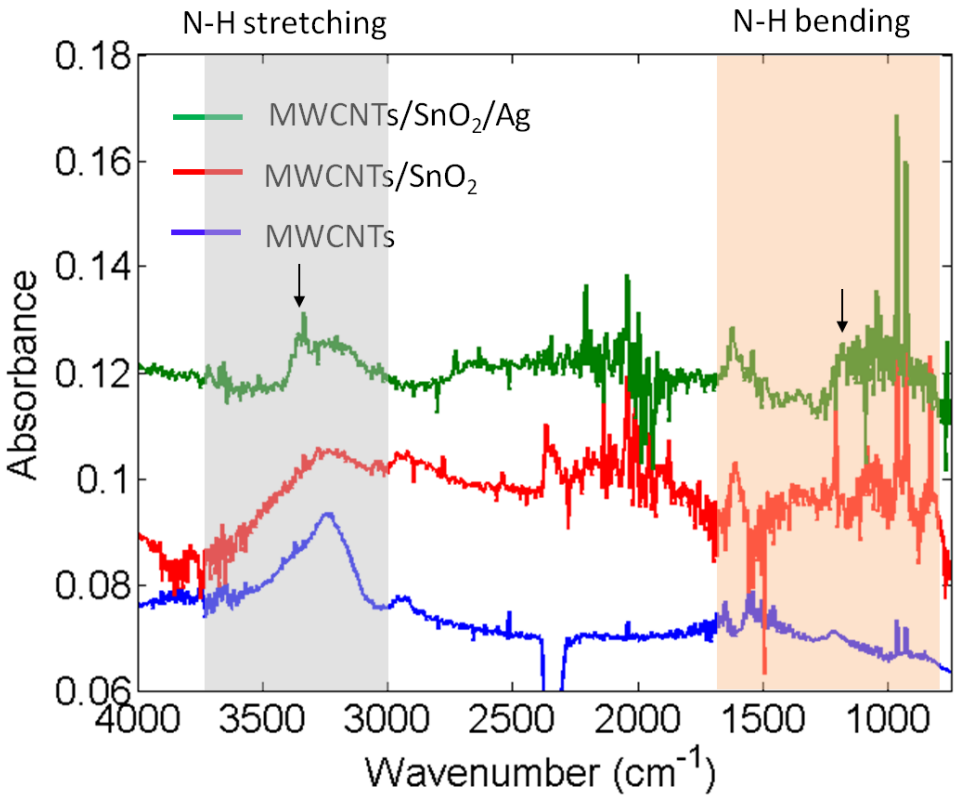

Fig. S8 Differential IR absorbance spectra of MWCNT hybrid sensors exposed to 1% NH_3 diluted in Ar. Spectra are scaled and offset for clarity. Features at 2,350 cm^{-1} and 1,400-1,800 cm^{-1} are due to incomplete cancellation of atmospheric CO_2 and water vapor, respectively. Gas-phase NH_3 rotation-vibration bands are present in the region

900-1,200 cm^{-1}. The MWCNT and MWCNT/SnO_2 spectra are quite similar, with only small difference between the two in the region 900-1,100 cm^{-1}.

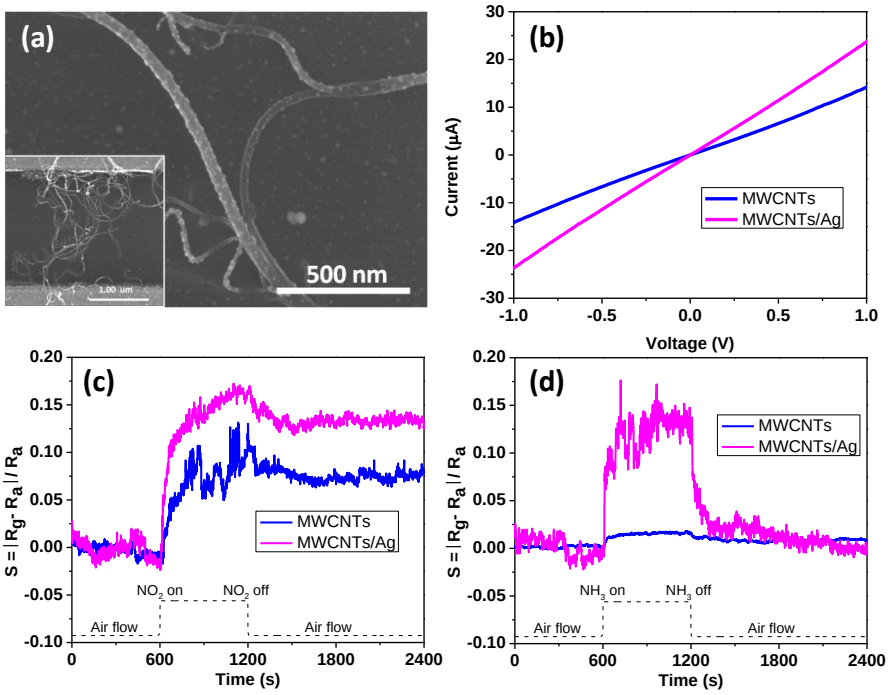

Fig. S9 (a) SEM image of MWCNTs coated with Ag NPs. Inset is an SEM image showing the hybrid structure bridging two gold electrodes. (b) I-V characteristics of MWCNTs and MWCNTs/Ag. (c) and (d) are sensing responses of bare MWCNTs and MWCNTs/Ag structures to 100 ppm NO_2 and 1% NH_3 at room temperature, respectively.

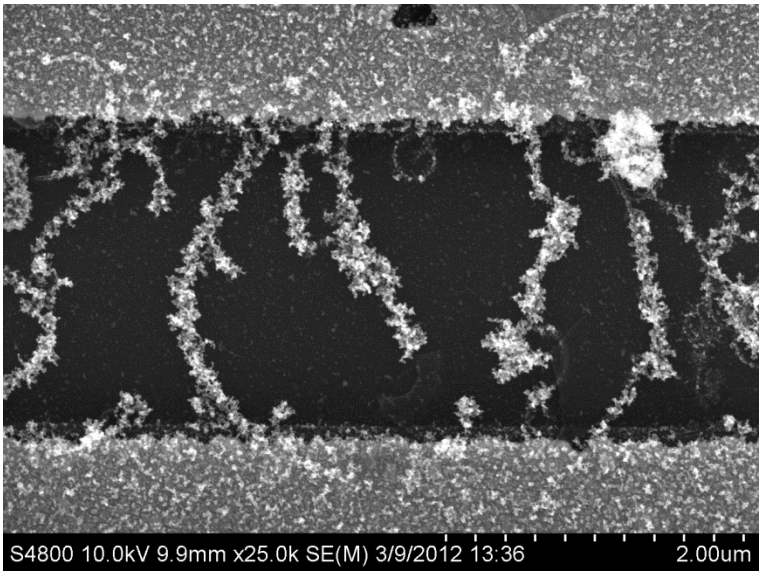

Fig. S10 SEM image of MWCNTs with full surface coverage of SnO_2 NPs

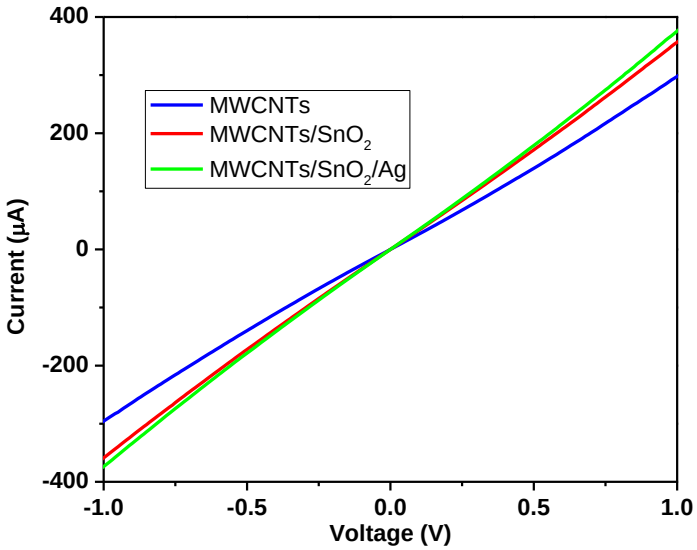

Fig. S11 *I-V* curve evolution of the control sample, which was obtained by first coating MWCNTs with SnO_2 NPs at a high coverage followed by additional coating of Ag NPs.